Spatially-Coupled Codes and Threshold Saturation on Intersymbol-Interference Channels

Phong S. Nguyen, Arvind Yedla, Henry D. Pfister, and Krishna R. Narayanan

Department of Electrical and Computer Engineering, Texas A&M University

College Station, TX 77840, U.S.A.

{psn, yarvind, hpfister, krn}@tamu.edu

Abstract

Recently, it has been observed that terminated low-density-parity-check (LDPC) convolutional codes (or spatially-coupled codes) appear to approach capacity universally across the class of binary memoryless channels. This is facilitated by the "threshold saturation" effect whereby the belief-propagation (BP) threshold of the spatially-coupled ensemble is boosted to the maximum a-posteriori (MAP) threshold of the underlying constituent ensemble.

In this paper, we consider the universality of spatially-coupled codes over intersymbol-interference (ISI) channels under joint iterative decoding. More specifically, we empirically show that threshold saturation also occurs for the considered problem. This can be observed by first identifying the EXIT curve for erasure noise and the GEXIT curve for general noise that naturally obey the general area theorem. From these curves, the corresponding MAP and the BP thresholds are then numerically obtained. With the fact that regular LDPC codes can achieve the symmetric information rate (SIR) under MAP decoding, spatially-coupled codes with joint iterative decoding can universally approach the SIR of ISI channels. For the dicode erasure channel, Kudekar and Kasai recently reported very similar results based on EXIT-like curves.

Index Terms

This material is based upon work supported by the National Science Foundation under Grant No. 0747470. The work of P. Nguyen was also supported in part by a Vietnam Education Foundation fellowship. Any opinions, findings, conclusions, or recommendations expressed in this material are those of the authors and do not necessarily reflect the views of the National Science Foundation.

Area theorem, BP threshold, EXIT curve, GEXIT curve, ISI channels, LDPC codes, MAP threshold, spatial coupling, symmetric information rate, threshold saturation.

I. INTRODUCTION

Irregular low-density parity-check (LDPC) codes can be carefully designed to achieve the capacity of the binary erasure channel (BEC) [1] and closely approach the capacity of general binary-input symmetric-output memoryless (BMS) channels [2] under belief-propagation (BP) decoding. LDPC convolutional codes, which were introduced in [3] and shown to have excellent BP thresholds in [4], [5], have recently been observed to *universally* approach the capacity of various channels. The fundamental mechanism behind this is explained well in [6], where it is proven analytically for the BEC that the BP threshold of a particular spatially-coupled ensemble converges to the maximum a-posteriori (MAP) threshold of the underlying ensemble. A similar result was also observed independently in [7] and stated as a conjecture. Such a phenomenon is now called "threshold saturation via spatial coupling" and has also been empirically observed for general BMS channels [8]. In fact, threshold saturation seems to be quite general and has now been observed in a wide range of problems, e.g., see [9], [10], [11], [12], [13], [14][1].

In the realm of channels with memory and particularly intersymbol interference (ISI) channels, the capacity may not be achievable via equiprobable signaling. For linear codes, a popular practice is to compare instead with the symmetric information rate (SIR), which is also known as $C_{\text{i.u.d.}}$ [15], because this the rate is achievable by random linear codes with maximum-likelihood (ML) decoding. A numerical method for tightly estimating the SIR of finite-state channels in general was first proposed in [16], [17]. For LDPC codes over ISI channels, a joint iterative BP decoder that operates on a large graph representing both the channel and the code constraints [18], [15] can perform quite well and even approach the SIR [19], [20]. Progress has been made on the design of SIR-approaching irregular LDPC codes for some specific ISI channels [19], [21], [22], [23], [20]. However, channel parameters must be known at the transmitter for such designs and therefore universality across ISI channels appears difficult to achieve.

Since spatially-coupled codes and the threshold saturation effect have now shown benefits in many communication problems, it is quite natural to consider them as a potential candidate to *universally* approach the SIR of ISI channels with low decoding complexity. In fact, the combination of spatially-coupled codes and ISI channels was recently considered by Kudekar and Kasai [11] for the simple dicode

[1]To be precise, the papers [9], [11], [12] only observe the threshold saturation effect indirectly because the considered EXIT-like curves provide no direct information about the MAP threshold of the underlying ensemble.

erasure channel (DEC) from [24], [20]. They provided a numerical evidence that the joint BP threshold of the spatially coupled codes can approach the SIR over the DEC (by increasing the degrees while keeping the rate fixed). Also, they outlined a tentative proof approach for the threshold saturation following the ideas in [6]. However, the EXIT-like curves they considered were not equipped with an area theorem and therefore could not be directly connected with the MAP threshold of the underlying ensemble. Thus, the threshold saturation effect was indirectly observed.

In this paper, we begin by considering the transmission of the spatially-coupled codes over the class of generalized erasure channels (GECs) of which the DEC and BEC are two particular examples. For these channels, we provide a rigorous analysis of the upper bound on the MAP threshold of LDPC codes by extending the analysis in [25] beyond the BEC case [2]. For the DEC, we then employ a counting argument and present a numerical evidence that this bound is indeed tight for regular ensembles. With the MAP threshold determined, the threshold saturation phenomenon can be observed to occur exactly for the several channels from the GECs. Next, we also consider the case of more general ISI channels where, by deriving the appropriate GEXIT curve and associated area theorem, the MAP threshold upper bound can be computed and threshold saturation can be seen. As a consequence, it is possible for spatially-coupled codes to closely approach the SIR of ISI channels under joint iterative BP decoding because regular LDPC codes can achieve the SIR under MAP decoding [27].

II. Background

In this section, we briefly describe our notation for ISI channels, LDPC ensembles, the joint iterative decoder and spatially-coupled codes.

A. ISI Channels and the SIR

Let the input alphabet $\mathcal{X}$ be finite, $\{X_i\}_{i\in\mathbb{Z}}$ be the discrete-time input sequence (i.e., $X_i \in \mathcal{X}$) and $\{Y_i\}_{i\in\mathbb{Z}}$ be the discrete-time output sequence. Many ISI channels of interest can be modeled by

$$Y_i = \sum_{t=0}^{\nu} a_t X_{i-t} + N_i, \tag{1}$$

where the channel memory is ν, $\{a_t\}_{t=1}^{\nu}$ is the set of tap coefficients and $\{N_i\}_{i\in\mathbb{Z}}$ is a sequence of independent noise random variables. One can also write the above as $Y_i = Z_i + N_i$ where $Z_i = \sum_{t=0}^{\nu} a_t X_{i-t}$ is the ISI output without noise. In this paper, we restrict ourself to the class of binary-input ISI channels.

[2]The upper bound technique on the MAP threshold for the DEC was first mentioned in an earlier paper by one of the authors [26]

Often, the tap coefficients are represented through a transform domain polynomial $a(D) = \sum_{t=0}^{\nu} a_t D^t$. For example, when $a(D) = 1 - D$, the channel is known as the dicode channel.

The main subject of Section III is the class of generalized erasure channels (GECs) in [24], [20]. For the GEC, one can evaluate its SIR (see [24], [20] for details) as

$$I_s(\epsilon) = 1 - \int_0^1 f(t, \epsilon) \mathrm{d}t \tag{2}$$

where $f(t, \epsilon)$ is the function which maps t, the *a priori* erasure rate from the code, and the channel erasure rate ϵ to the erasure rate at the output of the channel detector [20]. Strictly speaking, in this paper we mainly consider a subclass of the GECs where the channel output sequence can be modeled as a deterministic mapping of the input sequence plus erasure noise.

Example 1: The simpliest example is the dicode erasure channel (DEC), which is basically a 1st-order differentiator (i.e., $a(D) = 1 - D$) whose output is erased with probability ϵ and transmitted perfectly with probability $1 - \epsilon$. Furthermore, if the input bits are differentially encoded prior to transmission, the resulting channel is called the precoded dicode erasure channel (pDEC). The simplicity of the channel models allows one to analyze the recursions used by the Bahl-Cocke-Jelinek-Raviv (BCJR) algorithm [28] to compute

$$f_{\mathrm{DEC}}(t, \epsilon) = \frac{4\epsilon^2}{(2 - t(1 - \epsilon))^2} \tag{3}$$

for the DEC and

$$f_{\mathrm{pDEC}}(t, \epsilon) = \frac{4\epsilon^2 t(1 - \epsilon(1 - t))}{(1 - \epsilon(1 - 2t))^2} \tag{4}$$

for the pDEC. For both cases, explicit calculations give $I_s = 1 - \frac{2\epsilon^2}{1+\epsilon}$ [20]. Note that this formula also applies for the BEC where one has $f(t, \epsilon) = \epsilon$ and $I_s(\epsilon) = 1 - \epsilon$.

Section IV considers more general ISI channels among which the most important is probably linear ISI channels with additive white Gaussian noise (AWGN). For this class of ISI channels, the SIR is given by[3]

$$C_{\text{i.u.d.}} = \lim_{n \to \infty} \frac{1}{n} I(X_1^n; Y_1^n)\Big|_{p_{X_1^n}(x_1^n) = 2^{-n}}.$$

Unfortunately, no closed-form solutions for the SIR are known in this case. Instead, the numerical method described in [16], [17], [29] is typically used to give tight estimates of the SIR.

[3]A vector $(X_1, X_2, \ldots, X_n)$ is denoted by X_1^n for convenience.

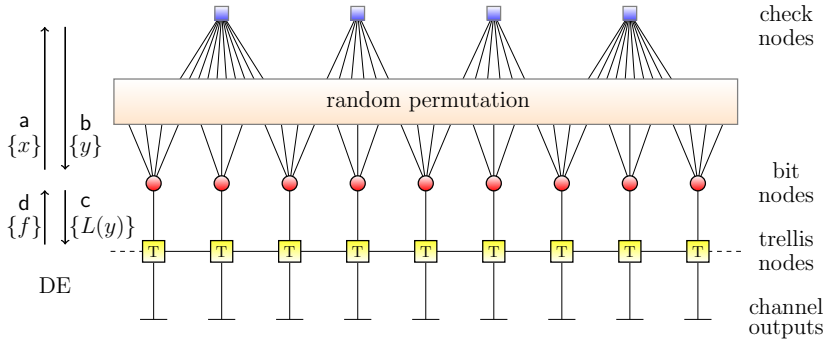

Figure 1. Gallager-Tanner-Wiberg graph of the joint BP decoder for ISI channels. The notations $\mathsf{a}, \mathsf{b}, \mathsf{c}, \mathsf{d}$ denote the average densities of the messages traversing along the graph used in density evolution (DE). The quantities inside the brackets are erasure rates used in DE for the GEC case. The update schedule of the joint BP decoder is also implied by the arrows in this figure.

B. LDPC Ensembles and the Joint BP Decoder

The standard irregular LDPC ensemble is characterized by its degree distribution (d.d.), which represents the fraction of nodes (or edges) of particular degrees. From the edge perspective, the d.d. pair consists of two polynomials $\lambda(x) = \sum_{i\geq 1} \lambda_i x^{i-1}$ and $\rho(x) = \sum_{i\geq 1} \rho_i x^{i-1}$ whose coefficients λ_i (or ρ_i) give the fraction of edges that connect to bit (or check) nodes of degree i. The LDPC ensemble can also be viewed from the node perspective where its d.d. pair $L(x) = \sum_{i\geq 1} L_i x^i$ and $R(x) = \sum_{i\geq 1} R_i x^i$ have coefficients L_i (or R_i) equal to the fraction of bit (or check) nodes of degree i. The design rate of an LDPC ensemble is given by

$$\mathtt{r} = 1 - \frac{L'(1)}{R'(1)} = 1 - \frac{\int_0^1 \rho(x)\mathrm{d}x}{\int_0^1 \lambda(x)\mathrm{d}x}.$$

When LDPC codes are transmitted over the ISI channels defined by (1), one can construct a large graph by joining the code graph and the channel graph together as depicted in Fig. 1. Working on this joint graph, a joint iterative decoder typically passes the information back and forth between the channel detector and the LDPC decoder. This technique is termed as turbo equalization and was first considered by Douillard *et al.* in the context of turbo codes [30]. For analysis, we also require the addition of a random scrambling vector to symmetrize the effective channel [31]. This is very similar to using a random coset of the LDPC code to allow analysis of the decoder using the all-zero codeword assumption; this technique was also used in [15] where they proved a concentration theorem and derived the density evolution (DE) equations for ISI channels.

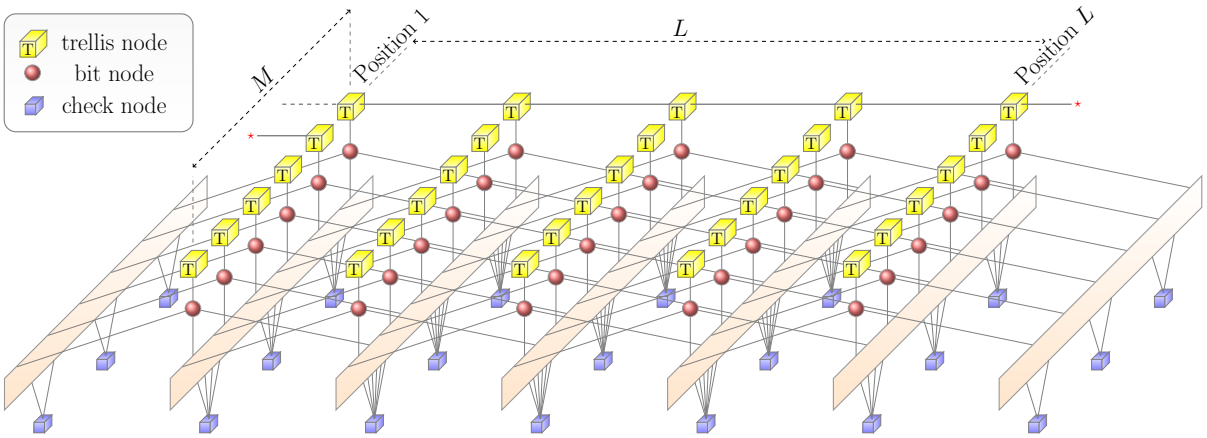

Figure 2. The joint graph for the (l, r, L) ensemble over the ISI channels. Illustrated in this figure is the case when $l = 3$ and $r = 6$.

C. Spatially-Coupled Ensembles

The class of spatially-coupled ensembles in general can be defined quite broadly. In this paper, we mainly consider two basic variants (see details in [6]) as discussed below.

1) The (l, r, L) ensemble: The (l, r, L) spatially-coupled ensemble (with l odd so that $\hat{l} = \frac{l-1}{2} \in \mathbb{N}$) can be constructed from the underlying (l, r)-regular LDPC ensemble. At each position from $[1, L]$ one has M bit nodes and $\frac{l}{r}M$ check nodes just like in the (l, r)-regular case. However, each bit node at position i is connected to check nodes at the same position, at $\hat{l}$ positions to the left and $\hat{l}$ positions to the right (one check node from each position). In doing this, one also needs to add $\frac{l}{r}M$ extra check nodes at each of $\hat{l}$ extra positions on each side. For example, a joint code/channel graph for the $(3, 6, L)$ ensemble and the ISI channels is shown in Fig. 2. The design rate of the (l, r, L) ensemble is given by

$$\mathtt{r}(l, r, L) = \left(1 - \frac{l}{r}\right) - \frac{l}{r} \cdot \frac{l-1}{L}.$$

2) The (l, r, L, w) ensemble: The (l, r, L, w) can be obtained with the introduction of a "smoothing" parameter w. One still places M variable nodes at each position in $[1, L]$ but places $\frac{l}{r}M$ check nodes at each position in $[1, L + w - 1]$. Each bit node at position i is connected uniformly and independently to a total of l check nodes at positions from the range $[i, i + w - 1]$. By adding this randomization of the edge connections with the parameter w, for large enough w the system behaves like a continuous one and a proof of the threshold saturation effect becomes feasible [6]. The design rate of the (l, r, L, w) ensemble

is given by

$$\mathtt{r}(l,r,L,w) = \left(1-\frac{l}{r}\right) - \frac{l}{r}\cdot\frac{w+1-2\sum_{i=0}^{w}\left(\frac{i}{w}\right)^{r}}{L}.$$

III. ISI Channels with Erasure Noise: The GECs

In this section, we focus on the class of GECs. We will present some closed-form analyses on the (E)BP EXIT curves of the joint BP decoder. This allows us to obtain an estimate of the MAP threshold of the underlying ensemble. Then, DE is used to computed the BP thresholds of the corresponding spatially-coupled ensembles and the threshold saturation effect is demonstrated.

A. BP and EBP Curves for the GEC

For the class of GECs, the DE update equation of the joint BP decoder is given by

$$x^{(\ell+1)} = f\big(L(1-\rho(1-x^{(\ell)}),\epsilon)\lambda(1-\rho(1-x^{(\ell)}))\big)$$

where $x^{(\ell)}$ is the average erasure rate emitted from bit nodes to check nodes during the ℓth iteration [20].

Let x denote the limit of $x^{(\ell)}$ when $\ell\to\infty$. The fixed point (FP) equation is then given by

$$x = f(L(y(x)),\epsilon)\lambda(y(x)) \tag{5}$$

where, for simplicity of notation, we use $y(x)\triangleq 1-\rho(1-x)$ (and sometimes y for short).

For most of the GECs, $f(t,\epsilon)$ is strictly increasing in ϵ for fixed t. In this case, there exists a unique function $\xi(t,v)$ such that $f(t,\xi(t,v)) = v$ and one can obtain

$$\epsilon(x) = \xi\left(L(y(x)),\frac{x}{\lambda(y(x))}\right). \tag{6}$$

Example 2: For the DEC case, one has $f(t,\epsilon) = \frac{4\epsilon^2}{(2-t(1-\epsilon))^2}$ and this gives the FP equation $x = \frac{4\epsilon^2\lambda(y)}{(2-L(y)(1-\epsilon))^2}$. One can also solve for $\xi(t,v) = (2-t)/\left(\frac{2}{\sqrt{v}}-t\right)$ and gets

$$\epsilon(x) = \frac{2-L(y(x))}{2\sqrt{\frac{\lambda(y(x))}{x}}-L(y(x))}. \tag{7}$$

Definition 1: Consider a d.d. (λ,ρ) pair and the sequence of LDPC ensembles LDPC(n,λ,ρ). For each $\mathcal{C}$ picked uniformly at random from LDPC(n,λ,ρ), let X_1^n be chosen randomly and uniformly at random from $\mathcal{C}$ and and Y_1^n be the received sequence after transmission over a GEC with erasure rate ϵ and initial state S_0. The associated EXIT function is defined as

$$h(\epsilon)\triangleq\lim_{n\to\infty}\mathbb{E}_{\mathcal{C}}\left[\frac{\partial H(X_1^n|Y_1^n(\epsilon),S_0)}{\partial\epsilon}\right].$$

When BP estimator is used at each bit instead of the optimal MAP estimator, one also has the BP-EXIT function which is given by the following definition.

Definition 2: Consider the same setting as in Definition 1, the associated (joint) BP-EXIT function is defined to be

$$h^{\mathrm{BP}}(\epsilon) \triangleq \lim_{\ell\to\infty} h^{\mathrm{BP},\ell}(\epsilon)$$

where

$$h^{\mathrm{BP},\ell}(\epsilon) = \lim_{n\to\infty} \mathbb{E}_{\mathcal{C}}\left[\frac{1}{n}\sum_{i=1}^{n}\frac{\partial H(X_1^n|Y_i(\epsilon),\mathcal{E}_i^{\mathrm{BP},\ell},S_0)}{\partial\epsilon}\right]$$

and $\mathcal{E}_i^{\mathrm{BP},\ell}$ is the extrinsic BP estimate of the ith bit after iteration ℓ.

Lemma 1: For simplicity of notation, let us write $Y_{\sim i}$ to denote the sequence $Y_1^n \setminus Y_i$. Then, the EXIT function and BP-EXIT function (after iteration ℓ) can be written as

$$h(\epsilon) = \lim_{n\to\infty} \mathbb{E}_{\mathcal{C}}\left[\frac{1}{n}\sum_{i=1}^{n} H(Z_i|Y_{\sim i}(\epsilon),S_0)\right], \tag{8}$$

$$h^{\mathrm{BP},\ell}(\epsilon) = \lim_{n\to\infty} \mathbb{E}_{\mathcal{C}}\left[\frac{1}{n}\sum_{i=1}^{n} H(Z_i|\mathcal{E}_i^{\mathrm{BP},\ell}(Y_{\sim i}(\epsilon)),S_0)\right]. \tag{9}$$

where Z_i is the ith output without noise. From this, one can see that $h(\epsilon) \le h^{\mathrm{BP}}(\epsilon)$.

Proof: Let ϵ_i be the erasure rate of the channel from Z_i to Y_i. For any extrinsic estimator $\mathcal{E}$, one has

$$\begin{aligned} H(X_1^n|Y_i(\epsilon_i),\mathcal{E}(Y_{\sim i}),S_0) &= H(Z_1^n|Y_i(\epsilon_i),\mathcal{E}(Y_{\sim i}),S_0) \\ &= H(Z_i|Y_i(\epsilon_i),\mathcal{E}(Y_{\sim i}),S_0) + H(Z_{\sim i}|Y_i(\epsilon_i),\mathcal{E}(Y_{\sim i}),Z_i,S_0) \\ &= \epsilon_i H(Z_i|\mathcal{E}(Y_{\sim i}),S_0) + H(Z_{\sim i}|Y_i(\epsilon_i),\mathcal{E}(Y_{\sim i}),Z_i,S_0). \end{aligned}$$

Since the second term on the R.H.S. does not depend on ϵ_i, it is clear that

$$\frac{\partial H(X_1^n|Y_i(\epsilon_i),\mathcal{E}(Y_{\sim i}),S_0)}{\partial\epsilon_i} = H(Z_i|\mathcal{E}(Y_{\sim i}),S_0).$$

By letting $\epsilon_i = \epsilon$ for all i and considering two specific cases of $\mathcal{E}$, one obtains (8) and (9).

Furthermore, by data processing inequality [32], one has $H(Z_i|Y_{\sim i}(\epsilon),S_0) \le H(Z_i|\mathcal{E}_i^{\mathrm{BP},\ell}(Y_{\sim i}(\epsilon)),S_0)$ which implies $h(\epsilon) \le h^{\mathrm{BP},\ell}(\epsilon)$ hence $h(\epsilon) \le h^{\mathrm{BP}}(\epsilon)$. ■

While computing the (MAP) EXIT function in general is hard, it is relatively easy to compute the BP-EXIT function.

Lemma 2: The BP-EXIT function for the GEC is given by

$$h^{\mathrm{BP}}(\epsilon) = \frac{\partial}{\partial\tilde{\epsilon}}\int_0^{L(y)} f(t,\tilde{\epsilon})\mathrm{d}t\Big|_{\tilde{\epsilon}=\epsilon}. \tag{10}$$

where $L(y)$ is the extrinsic erasure rate given by the FP equation at channel erasure rate ϵ.

Proof: Let $Y_1^n(\tilde{\epsilon})$ be the result of passing X_1^n through the communication channel, e.g., the GEC, with erasure rate $\tilde{\epsilon}$ and, with some abuse of notation, $\mathcal{E}_1^n(p)$ be the result of passing X_1^n through the extrinsic channel which is modeled as BEC with erasure probability p. Similarly to [20], let $T_n(1-t,\tilde{\epsilon}) \triangleq \frac{1}{n}\sum_{i=1}^n I(X_i; Y_1^n(\tilde{\epsilon}), \mathcal{E}_{\sim i}(p))$ denote the mutual information transfer function where $\mathcal{E}_{\sim i}$ comprises the sequence of extrinsic bit estimates except for the ith bit. We also let $f_n(t,\tilde{\epsilon}) \triangleq 1 - T_n(1-t,\tilde{\epsilon})$. By the area theorem [33], [25, Th. 2], one obtains

$$\int_0^\delta \frac{1}{n}\sum_{i=1}^n H(X_i|Y_1^n(\epsilon), \mathcal{E}_{\sim i}(t))\mathrm{d}t = \frac{1}{n}H(X_1^n|Y_1^n(\epsilon), \mathcal{E}_1^n(\delta)). \tag{11}$$

We then have

$$\begin{aligned}
\frac{\partial}{\partial\tilde{\epsilon}}\int_0^\delta f_n(t,\tilde{\epsilon})\mathrm{d}t &= -\frac{\partial}{\partial\tilde{\epsilon}}\int_0^\delta T_n(1-t,\tilde{\epsilon})\mathrm{d}t \\
&= \frac{\partial}{\partial\tilde{\epsilon}}\int_0^\delta \left(-\frac{1}{n}\sum_{i=1}^n I(X_i; Y_1^n(\tilde{\epsilon}), \mathcal{E}_{\sim i}(t))\right)\mathrm{d}t \\
&= \frac{\partial}{\partial\tilde{\epsilon}}\int_0^\delta \left(\frac{1}{n}\sum_{i=1}^n H(X_i) - \frac{1}{n}\sum_{i=1}^n I(X_i; Y_1^n(\tilde{\epsilon}), \mathcal{E}_{\sim i}(t))\right)\mathrm{d}t \qquad (12) \\
&= \frac{\partial}{\partial\tilde{\epsilon}}\int_0^\delta \frac{1}{n}\sum_{i=1}^n H(X_i|Y_1^n(\tilde{\epsilon}), \mathcal{E}_{\sim i}(t))\mathrm{d}t \\
&= \frac{\partial}{\partial\tilde{\epsilon}}\left[\frac{1}{n}\sum_{i=1}^n H(X_1^n|Y_1^n(\tilde{\epsilon}), \mathcal{E}_1^n(\delta))\right] \qquad (13)
\end{aligned}$$

where (12) holds because $\frac{\delta}{n}\sum_{i=1}^n H(X_i)$ is not a function of $\tilde{\epsilon}$ while (13) follows from (11).

If one considers the BP estimator, for each fixed ℓ, by letting $n \to \infty$, $f_n(t,\tilde{\epsilon})$ converges pointwise to $f(t,\tilde{\epsilon})$ (see [20]) while the expectation of the R.H.S. of (13) converges to $h^{\mathrm{BP},\ell}(\epsilon)$ if we choose $\epsilon = \tilde{\epsilon}$. Then, by letting $\ell \to \infty$, one reaches a FP where $\delta \to L(y)$ and finally obtains

$$\frac{\partial}{\partial\tilde{\epsilon}}\int_0^{L(y)} f_n(t,\tilde{\epsilon})\mathrm{d}t\Big|_{\tilde{\epsilon}=\epsilon} = h^{\mathrm{BP}}(\epsilon).$$

■

Example 3: For the DEC and pDEC, using the result of (3) and (4), one has the following BP-EXIT functions

$$\begin{aligned}
h_{\mathrm{DEC}}^{\mathrm{BP}}(\epsilon) &= \frac{\partial}{\partial\tilde{\epsilon}}\int_0^{L(y)} \frac{4\tilde{\epsilon}^2}{(2-t(1-\tilde{\epsilon}))^2}\mathrm{d}t\Big|_{\tilde{\epsilon}=\epsilon} \\
&= \frac{2\epsilon L(y)(4-L(y)(2-\epsilon))}{(2-L(y)(1-\epsilon))^2} \qquad (14)
\end{aligned}$$

and

$$h_{\text{pDEC}}^{\text{EBP}}(\epsilon) = \frac{\partial}{\partial\tilde{\epsilon}}\int_0^{L(y)} \frac{4\tilde{\epsilon}^2 t(1-\tilde{\epsilon}(1-t))}{(1-\tilde{\epsilon}(1-2t))^2}\mathrm{d}t\Big|_{\tilde{\epsilon}=\epsilon}$$
$$= \frac{2\epsilon L^2(y)(2-\epsilon(1-2L(y)))}{(1-\epsilon(1-2L(y)))^2}.$$

where x is the DE FP at channel erasure rate ϵ and $y = y(x)$. The formula (14) for the DEC case is equivalent to the result shown in [26] by analyzing the BCJR algorithm.

Also, one can apply (10) for the BEC to obtain a known result $h_{\text{BEC}}^{\text{BP}}(\epsilon) = \frac{\partial}{\partial\tilde{\epsilon}}\int_0^{L(y)} \tilde{\epsilon}\mathrm{d}t\Big|_{\tilde{\epsilon}=\epsilon} = L(y)$. Using an approach similar to [25, Sec. III-B] and taking care of (6) and (10), one gets the following parametric form for the BP-EXIT function. This involves in defining

$$\mathcal{I} \triangleq \bigcup_{i\in[J]} [\underline{x}^i, \overline{x}^i) \cup \{1\}$$

as the unique finite union of disjoint intervals that represent all stable and achievable FPs of DE equations. Please note that J represents the number of discontinuties in the BP-EXIT function. For the case $J \geq 1$, let $x^{\text{BP}} = \underline{\text{x}}^1$ and $\epsilon^{\text{BP}} = \epsilon(x^{\text{BP}})$ is the joint BP decoding threshold [25, Sec. III-B].

Lemma 3: Given a d.d. pair (λ, ρ), the BP-EXIT function for the GEC is given parametrically as follows

$$\left(\epsilon, h^{\text{BP}}(\epsilon)\right) = \begin{cases} (\epsilon, 0), & \epsilon \in [0, \epsilon^{\text{BP}}) \\ \left(\epsilon(x), \frac{\partial}{\partial\tilde{\epsilon}}\int_0^{L(y(x))} f(t,\tilde{\epsilon})\mathrm{d}t\Big|_{\tilde{\epsilon}=\epsilon(x)}\right) \ \forall x \in \mathcal{I}, & \epsilon \in (\epsilon^{\text{BP}}, 1] \end{cases}$$

where $\epsilon(x)$ is given in (6).

In [25], the extended BP (EBP) EXIT curve for the BEC was introduced as the hidden bridge between the BP threshold and its MAP counterpart. In a similar manner, the EBP-EXIT curve for the GEC is given below with its own area theorem.

Definition 3: For a given d.d. pair (λ, ρ), the EBP-EXIT curve for the GEC is defined by the pair

$$\left(\epsilon(x), \frac{\partial}{\partial\tilde{\epsilon}}\int_0^{L(y(x))} f(t,\tilde{\epsilon})\mathrm{d}t\Big|_{\tilde{\epsilon}=\epsilon(x)}\right), \ x \in [0,1]$$

where $\epsilon(x)$ is given in (6).

Example 4: For the DEC case, using (7) and (14), the EBP-EXIT curve is given by

$$\left(\frac{2-L(y(x))}{2\sqrt{\frac{\lambda(y(x))}{x}} - L(y(x))}, L(y(x))\left(2\sqrt{\frac{x}{\lambda(y(x))}} - \frac{xL(y(x))}{2\lambda(y(x))}\right)\right), \ x \in [0,1].$$

Lemma 4: Consider the GEC and a d.d. pair (λ, ρ). Define the "trial entropy" as

$$P(x) \triangleq \int_0^x h^{\text{EBP}}(t)\epsilon'(t)\mathrm{d}t$$

where $h^{\text{EBP}}(x)$ is the second coordinate the EBP-EXIT curve. Then, we have

$$P(x) = \int_0^{L(y)} f(t,\epsilon(x))\mathrm{d}t - \frac{L'(1)}{R'(1)}(1-R(1-x)-xR'(1-x)). \tag{15}$$

Proof: First, we let

$$\begin{aligned} Q(x) &\triangleq \int_0^{L(y)} f(t,\epsilon(x))\mathrm{d}t - \frac{L'(1)}{R'(1)}(1-R(1-x)-xR'(1-x)) \\ &= \int_0^{L(y)} f(t,\epsilon(x))\mathrm{d}t - L'(1)\int_0^x u\mathrm{d}y(u) \end{aligned} \tag{16}$$

where in (16), integration by parts is used.

Then, one can use Leibniz's rule to get

$$\begin{aligned} Q'(x) &= f(L(y),\epsilon(x))y'L'(y) + \int_0^{L(y)} \frac{\partial}{\partial x} f(t,\epsilon(x))\mathrm{d}t - L'(1)xy' \\ &= \int_0^{L(y)} \frac{\partial}{\partial x} f(t,\epsilon(x))\mathrm{d}t \qquad (17) \\ &= \int_0^{L(y)} \frac{\partial}{\partial \epsilon(x)} f(t,\epsilon(x))\frac{\mathrm{d}}{\mathrm{d}x}\epsilon(x)\mathrm{d}t \\ &= \epsilon'(x)\int_0^{L(y)} \frac{\partial}{\partial \epsilon(x)} f(t,\epsilon(x))\mathrm{d}t \\ &= \epsilon'(x)h^{\text{EBP}}(x) \\ &= P'(x) \qquad (18) \end{aligned}$$

where (17) follows from the DE equation $f(L(y),\epsilon(x))\lambda(y) = x$ and the fact that $\lambda(y) = \frac{L'(y)}{L'(1)}$ while (18) follows by taking deravative.

Thus, $Q(x)$ and $P(x)$ may differ by a constant. By seeing that $P(0) = Q(0) = 0$, one must have $P(x) \equiv Q(x)$. ■

Example 5: For the DEC, explicit calculation gives

$$P(x) = \frac{2\epsilon^2(x)L(y)}{2-L(y)(1-\epsilon(x))} - \frac{L'(1)}{R'(1)}(1-R(1-x)-xR'(1-x)).$$

Also, one can see that, for the BEC, this gives same formula as in [25].

Theorem 1: (Area Theorem for EBP) Consider a d.d. pair (λ,ρ) of design rate $\mathtt{r}$. Then the EBP EXIT curve for the GEC satisfies

$$\int_0^1 h^{\text{EBP}}(x)\mathrm{d}\epsilon(x) = \mathtt{r}.$$

Proof: Using the result in Lemma 4, a direct calculation reveals that

$$\int_0^1 h^{\text{EBP}}(x)\mathrm{d}\epsilon(x) = P(1) = \int_0^1 f(t,1)\mathrm{d}t - \frac{L'(1)}{R'(1)} = 1 - \frac{L'(1)}{R'(1)} = \mathtt{r}$$

and the theorem is proven. ■

B. Upper Bound on the MAP Threshold

Because of the optimality of the MAP decoder in the sense that $h^{\text{MAP}} \leq h^{\text{BP}}$ (see Lemma 1), one can obtain an upper bound on the MAP threshold by first finding the largest value x^{MAP} such that $\int_{x^{\text{MAP}}}^{1} h^{\text{EBP}}(x)\mathrm{d}\epsilon(x) = \mathtt{r}$ and then bound the MAP threshold by the inequality $\epsilon^{\text{MAP}} \leq \bar{\epsilon}^{\text{MAP}} \triangleq \epsilon(x^{\text{MAP}})$. This technique was introduced by Méasson *et al.* in [25] in the context of BEC and conjectured to be tight in many scenarios. In fact, for the whole class of regular LDPC ensembles over the BEC, this bound was analytically proven to be tight [34].

With the ingredients provided in our analysis above, the technique can also be extended to the whole class of GECs. A corollary of Lemma 4 implies in a few steps that one can find x^{MAP} as the unique solution of $P(x) = 0$ in $[x^{\text{BP}}, 1]$. From this, it is also clear that, $\bar{\epsilon}^{\text{MAP}}$ for the case of regular LDPC ensembles quickly approaches ϵ^{SIR} of the GEC which is formalized by the following theorem.

Theorem 2: Consider the (l, r)-regular ensemble. Consider a fixed design rate $\mathtt{r} = 1 - \frac{l}{r}$. Then

$$\lim_{l,r\to\infty,\,\mathtt{r}\text{ fixed}} \bar{\epsilon}^{\text{MAP}}(l, r) = \epsilon^{\text{SIR}}(\mathtt{r})$$

where $\epsilon^{\text{SIR}}(\mathtt{r})$ is the corresponding erasure rate when SIR defined in (2) equals $\mathtt{r}$.

Proof: First, $x^{\text{MAP}}(l, r)$ must be the solution of $P(x) = 0$. For a fixed rate $\mathtt{r}$, $x^{\text{MAP}}(l, r)$ is bounded away from zero for l large enough (one can show that $x^{\text{MAP}}(l, r)$ for the GEC is not less than $x^{\text{MAP}}_{\text{BEC}}(l, r)$ for the BEC and the latter converges to $1 - \mathtt{r}$ [6, Lm. 8]). Suppose that all the limits are taken when $l, r \to \infty$ while $\mathtt{r}$ is kept fixed. Then, we have $(1 - x^{\text{MAP}}(l, r))^{r-1} \to 0$ exponentially fast.

Next, one also sees that

$$L(y(x^{\text{MAP}}(l, r))) = (1 - (1 - x^{\text{MAP}}(l, r))^{r-1})^{l} \to 1 \text{ and } \lambda(y(x^{\text{MAP}}(l, r))) \tag{19}$$

which can be obtained from

$$\frac{\log\left(1 - (1 - x^{\text{MAP}}(l, r))^{r-1}\right)}{1/(r-1)} \to 0. \tag{20}$$

To see (20), we apply L'Hôpital's rule and use the fact that

$$\frac{(1 - x^{\text{MAP}}(l, r))^{r-1}}{(1 - (1 - x^{\text{MAP}}(l, r))^{r-1}))\,/(r-1)^2} \to 0$$

because the numerator vanishes exponentially while the denominator only vanishes quadratically fast.

Note that for (l, r)-regular ensemble, (15) can be rewritten as

$$P(x) = \int_0^{L(y)} f(t, \epsilon(x))\mathrm{d}t + \frac{l}{r}(1 - x)^{r-1}(1 + (r-1)x) - \frac{l}{r} = 0. \tag{21}$$

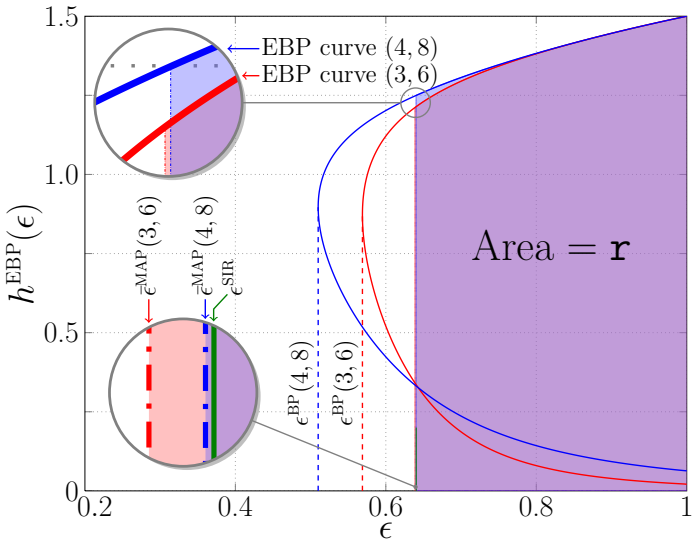

Figure 3. EBP EXIT curves for $(3,6)$ and $(4,8)$ regular LDPC ensembles over the DEC. Projection of the left most point of the curves on to the ϵ-axis allows one to determine ϵ^{BP}. Setting the area under the EBP curves to be equal to the design rate $\mathtt{r}$ can help find $\bar{\epsilon}^{\mathrm{MAP}}$.

Therefore, we can use $P(x^{\mathrm{MAP}}(l,r)) = 0$ and (21), (19) to have

$$\int_0^1 f(t, \epsilon(x^{\mathrm{MAP}}(l,r)))\mathrm{d}t \to \frac{l}{r} = 1 - \mathtt{r}.$$

In addition, from definition we have $\int_0^1 f(t, \epsilon^{\mathrm{SIR}}(\mathtt{r}))\mathrm{d}t = 1 - I_s(\epsilon^{\mathrm{SIR}}(\mathtt{r})) = 1 - \mathtt{r}$. Therefore,

$$I_s(\bar{\epsilon}^{\mathrm{MAP}}(l,r)) \to I_s(\epsilon^{\mathrm{SIR}}(\mathtt{r}))$$

and one has $\bar{\epsilon}^{\mathrm{MAP}}(l,r) \to \epsilon^{\mathrm{SIR}}(\mathtt{r})$ as $I_s(\cdot)$ is a continuous and monotone function. ■

Example 6: Let us consider the DEC. For rate one-half ensembles, we have $\bar{\epsilon}^{\mathrm{MAP}}(3,6) \approx 0.638659$, $\bar{\epsilon}^{\mathrm{MAP}}(4,8) \approx 0.640163$, $\bar{\epsilon}^{\mathrm{MAP}}(5,10) \approx 0.640355$, $\bar{\epsilon}^{\mathrm{MAP}}(7,14) \approx 0.640387$, $\bar{\epsilon}^{\mathrm{MAP}}(8,16) \approx 0.640388$ that quickly approach $\epsilon^{\mathrm{SIR}}(\frac{1}{2}) \approx 0.640388$. This can be partially seen in Fig. 3 where $\bar{\epsilon}^{\mathrm{MAP}}(4,8)$ is already very close to ϵ^{SIR}.

C. Tightness of the upper bound

In this section, we discuss the tightness of the $\bar{\epsilon}^{\mathrm{MAP}}$ bounding technique. Assume that the joint BP decoder is run on the joint graph of the LDPC code and GEC. Since one never gets errors in the GEC, the joint BP decoder must reach a FP where no more bit nodes can be decoded. At this FP, one obtains a residual graph (see [35, Ch. 3]) by removing all the known bit nodes as well as their neighboring check

nodes and the edges connecting them. Then, one can follow the general procedure to show that the MAP bounding technique is tight, i.e., by seeing at channel erasure rate $\bar{\epsilon}^{\text{MAP}}$, the design rate of the residual graph is zero and providing numerical evidence that for this residual graph, the actual rate converges to the design rate as the blocklength $n \to \infty$.

We start with the following lemma.

Lemma 5: Consider a d.d. pair (λ, ρ) and the GEC with channel erasure rate ϵ. First, run the joint BP decoder until it reaches a FP so that we obtain a residual graph. Next, use the remaining channel constraints to merge all bit nodes that must have the same value. The expected check node d.d. of the residual graph[4] is given by

$$\tilde{R}_\epsilon(z) = R(1-x+zx) - R(1-x) - zxR'(1-x) \tag{22}$$

where x is the FP of DE and $y = 1-\rho(1-x)$. Furthermore, if the expected bit node d.d. is

$$\tilde{L}_\epsilon(z) = \int_0^{L(yz)} f(t,\epsilon)\mathrm{d}t \tag{23}$$

then at $\epsilon = \bar{\epsilon}^{\text{MAP}}$, the design rate of the residual graph $\tilde{\mathtt{r}}_{\bar{\epsilon}^{\text{MAP}}}$ equals zero.

Proof: Consider the original graph at the FP and let x be the average erasure rate from a bit node to a check node. Pick a check node of degree j in the original graph. We can obtain a check node of degree $i \le j$ in the residual graph by removing all $(j-i)$ edges with known values. Note that $i \ge 2$ since a check node of degree one must not be in the residual graph. The remaining i edges of this check node must contain erasure messages. The probability for this event is $\binom{j}{i}(1-x)^{(j-i)}x^i$. Thus, the check node d.d. for the residual graph (normalized by the number of check nodes in the original graph) is[5]

$$\begin{aligned}\tilde{R}_\epsilon(z) &= \sum_{j\ge 2} R_j \sum_{i=2}^{j} \binom{j}{i}(1-x)^{(j-i)}(xz)^i \\ &= R(1-x+zx) - R(1-x) - zxR'(1-x)\end{aligned}$$

and (22) holds.

Suppose the bit node d.d. is given by (23), one has $\tilde{L}'_\epsilon(z) = y'L'(yz)f(L(yz),\epsilon)$ and $\tilde{R}'_\epsilon(z) =$

[4]The check node and bit node d.d. are normalized with respect to the original graph.

[5]This formula is the same as the check node d.d. for residual graph left by the peeling decoder for the BEC, obtained via solving a differential equation in [1].

$xR'(1-x+zx) - xR'(1-x)$. Therefore, one obtains

$$\begin{aligned}\frac{\tilde{L}'_\epsilon(1)}{\tilde{R}'_\epsilon(1)} &= \frac{yL'(y)f(L(y),\epsilon)}{xR'(1)(1-\rho(1-x))} \\ &= \frac{L'(1)}{R'(1)} \cdot \frac{\lambda(y)f(L(y),\epsilon)}{x} \\ &= \frac{L'(1)}{R'(1)} \end{aligned} \tag{24}$$

by using (5), $y = 1-\rho(1-x)$ and the known facts that $L'(y) = L'(1)\lambda(y)$ and $R'(1-x) = R'(1)\rho(1-x)$.

Note that the standard d.d. pair from the node perspective of the residual graph is $\left(\frac{\tilde{L}_\epsilon(z)}{\tilde{L}_\epsilon(1)}, \frac{\tilde{R}_\epsilon(z)}{\tilde{R}_\epsilon(1)}\right)$ and the corresponding design rate is then

$$\tilde{\mathtt{r}}_\epsilon = 1 - \frac{\tilde{L}'_\epsilon(1)}{\tilde{R}'_\epsilon(1)} \cdot \frac{\tilde{R}_\epsilon(1)}{\tilde{L}_\epsilon(1)}.$$

Using (24), it now is clear that

$$\tilde{\mathtt{r}}_\epsilon = 1 - \frac{L'(1)}{R'(1)} \cdot \frac{\tilde{R}_\epsilon(1)}{\tilde{L}_\epsilon(1)} = \frac{P(x)}{\tilde{L}_\epsilon(1)}$$

where the last equality follows from (22), (23) and (15).

By considering a special case $\epsilon = \bar{\epsilon}^{\text{MAP}}$, one has $\tilde{\mathtt{r}}_{\bar{\epsilon}^{\text{MAP}}} = P(x^{\text{MAP}})/\tilde{L}_{\bar{\epsilon}^{\text{MAP}}}(1) = 0$. ■

Remark 1: For the BEC, the bit node d.d. given in (23) matches the known result in [35, Th. 3.106]. In fact, this also holds for the DEC case which can be shown by the following lemma.

Lemma 6: Consider a d.d. pair (λ, ρ) and the DEC with erasure probability ϵ. The expected bit node d.d. in this case follows the form (23), i.e.,

$$\tilde{L}_\epsilon(z) = \frac{2\epsilon^2 L(yz)}{2 - L(yz)(1-\epsilon)} = \sum_{k=0}^{\infty} \epsilon^2 \left(\frac{1-\epsilon}{2}\right)^k L(yz)^{k+1} \tag{25}$$

Consequently, at $\epsilon = \bar{\epsilon}^{\text{MAP}}$ the design rate of the residual graph equals zero.

Proof: The bit nodes in the residual graph must connect to the trellis section of the form depicted in Fig. 4 for some $k \in \mathbb{N}$ (otherwise, the joint BP decoder can still decode).

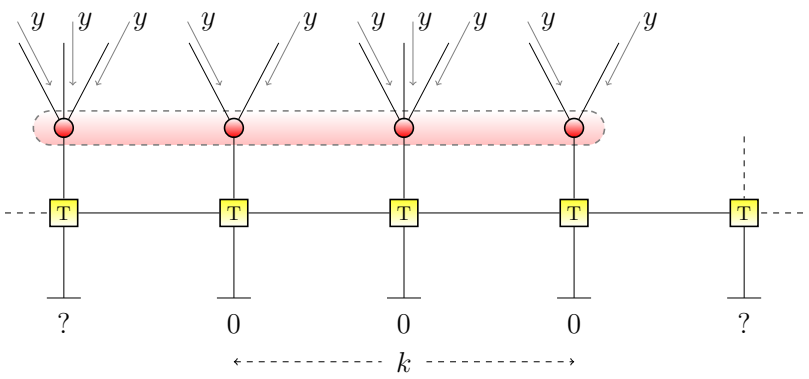

Figure 4. A trellis section in the residual graph for the DEC. The notation "?" denotes that an erasure is received at the channel output. One can form a larger bit node by merging all the bit nodes that attach to this trellis section.

The probability of the trellis configuration $(?, \overbrace{0, \ldots, 0}^{k}, ?)$, where $?$ indicates an erasure, is $\epsilon^2 \left(\frac{1-\epsilon}{2}\right)^k$. Given the above trellis configuration, if all messages from check nodes to the bit nodes that attach to this trellis section are "?" then *all* these bit nodes remain in the residual graph. On the other hand, if at least one of the messages is not "?", then the joint BP decoder can decode and then remove *all* these bit nodes from the residual graph. Therefore, one can consider all the bit nodes that attach to such a trellis section as one larger bit node whose degree is the sum of the $k+1$ component degrees. The generating function for this sum of $k+1$ i.i.d. random variables is $L(z)^{k+1}$. This is quite similar to the graph reduction technique discussed in [36] for IRA/ARA codes.

From the above analysis and since each edge is associated with erasure rate y, the d.d. (normalized by the number of bit nodes in the original graph) of residual graph after graph reduction is then given by

$$\tilde{L}_\epsilon(z) = \sum_{k=0}^{\infty} \epsilon^2 \left(\frac{1-\epsilon}{2}\right)^k L(yz)^{k+1} = \frac{2\epsilon^2 L(yz)}{2 - L(yz)(1-\epsilon)}.$$

■

From the above analysis, once one has $\tilde{\mathrm{r}}_{\bar{\epsilon}^{\mathrm{MAP}}} = 0$, the final missing piece to prove the tightness of the MAP upper bound is to show that the actual rate of the residual graph is equal to its design rate with high probability (when the blocklength tends to ∞)[6]. While a general proof for this still requires some analytic work, one can use the test in [35, Lm. 3.22] to numerically verify if this is true. To do this, one just needs to show that the function $\Psi(u)$ introduced in [35, Lm. 3.22], for the residual graph, has the following property: $\Psi(u) \leq 0$ in the interval $[0,1]$ with equality only at $u = 0$ and $u = 1$. For our case,

[6]If this is true, then the MAP decoder can decode perfectly at $\bar{\epsilon}^{\mathrm{MAP}}$ and $\bar{\epsilon}^{\mathrm{MAP}} = \epsilon^{\mathrm{MAP}}$.

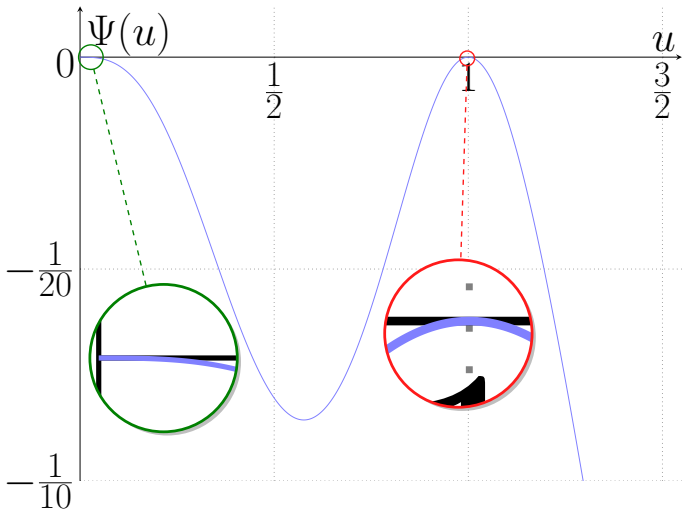

Figure 5. Function $\Psi(u)$ for the residual graph obtained after joint BP decoding of the $(3,6)$-regular LDPC ensemble over the DEC. This shows numerically that the MAP upper bound is tight in this case.

the bit node d.d. for the residual graph from (23) might have unbounded degrees as in (25) for the DEC case. However, for this DEC case, since the fraction of bit nodes, for the (l,r)-regular ensemble, that have degree $l(k+1)$ is upper bounded by $(\frac{1}{2})^k$ and therefore $\tilde{L}_\epsilon(z)$ has an exponentially vanishing tail, one can truncate the series $\tilde{L}_\epsilon(z)$ at some large enough k and obtain the result with a negligible error. For example, one can truncate $\tilde{L}_\epsilon(z)$ at $k = 20$ and for the $(3,6)$-regular ensemble, the truncated version of $\Psi(u)$ is numerically shown to satisfy the desired property in Fig. 5.

D. Spatially-Coupled Codes for the GEC

Consider the (l,r,L,w) spatially-coupled ensemble over the GEC. The joint code/channel graph is similar to the one in Fig. 2 which is for the (l,r,L) ensemble. We also follow the DE equation discussed in [11] to compute the BP thresholds of the coupled ensembles. The main difference is that we use the correct EBP curves with their operational meaning instead of the EXIT-like ones used in [11]. Let $x_i^{(\ell)}$ denote the expected erasure rate at iteration ℓ from bit nodes at position i to check nodes. For $i \notin [1,L]$, set $x_i^{(\ell)} = 0$. Let us define

$$g(x_{i-w+1},\dots,x_{i+w-1}) \triangleq \left(1-\frac{1}{w}\sum_{j=0}^{w-1}\left(1-\frac{1}{w}\sum_{k=0}^{w-1}x_{i+j-k}\right)^{r-1}\right)^{l-1},$$

$$\Gamma(x_{i-w+1},\dots,x_{i+w-1}) \triangleq \left(1-\frac{1}{w}\sum_{j=0}^{w-1}\left(1-\frac{1}{w}\sum_{k=0}^{w-1}x_{i+j-k}\right)^{r-1}\right)^{l}.$$

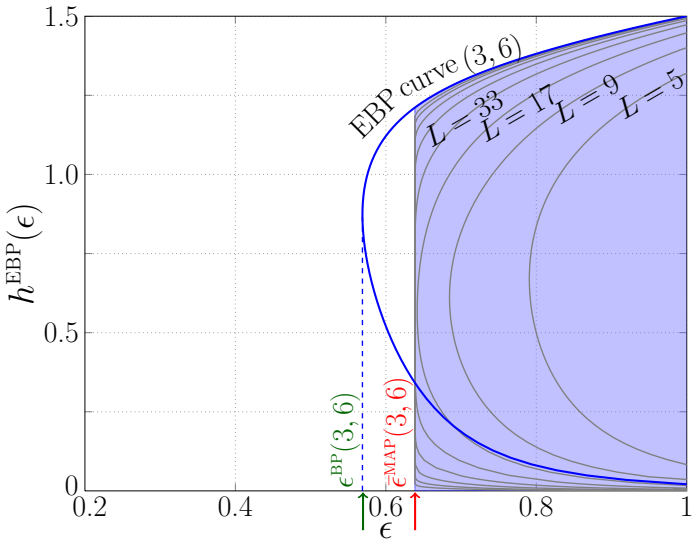

Figure 6. EBP EXIT curves for $(3,6,L,5)$ over the DEC with $L = 2\hat{L}+1$ where $\hat{L} = 2,4,8,16,32,64,128,246$. For small values of L, the increase in threshold can be explained by the large rate-loss. As L grows larger, the rate loss becomes negligible and the curves keep moving left, but they saturate at the MAP threshold of the underlying regular ensemble.

The DE equation for the joint BP decoder can be written as

$$x_i^{(\ell+1)} = f(\Gamma(x_{i-w+1}^{(\ell)},\ldots,x_{i+w-1}^{(\ell)}),\epsilon)\cdot g(x_{i-w+1}^{(\ell)},\ldots,x_{i+w-1}^{(\ell)})$$

for $i \in [1,L]$. To compute both the stable and unstable FPs of DE, one can use the fixed entropy DE procedure outlined in [37, Sec. VIII] where the normalized entropy of a constellation $\underline{x}^{(\ell)} = (x_1^{(\ell)},\ldots,x_L^{(\ell)})$, which is defined as $\chi(\underline{x}^{(\ell)}) = \frac{1}{L}\sum_{i=1}^{L} x_i^{(\ell)}$, is kept constant at every iteration by varying the channel parameter. With each FP $\underline{x}$ obtained, one can compute the EBP EXIT value of the spatially-coupled ensemble as $\frac{1}{L}\sum_{i=1}^{L} h^{\mathrm{EBP}}(x_i)$.

The threshold saturation effect of coupling can be nicely seen by plotting the EBP EXIT curves for the uncoupled and coupled codes. For the DEC, Fig. 6 shows the EBP curves for the $(3,6,L,5)$ ensembles with various L along with the EBP curve of the underlying $(3,6)$-regular ensemble. From the EBP curves, one can determine $\epsilon^{\mathrm{BP}}(3,6) \approx 0.56892$ and $\bar{\epsilon}^{\mathrm{MAP}}(3,6) \approx 0.63866$. The BP thresholds of spatially-coupled ensembles for small L due to rate-loss can have larger values, e.g., $\epsilon^{\mathrm{BP}}(3,6,17,6) \approx 0.64170 > \bar{\epsilon}^{\mathrm{MAP}}(3,6)$. However, for a wide range of L, i.e., $L = 33,65,129,257,513$, we observe that $\epsilon^{\mathrm{BP}}(3,6,L,5) \approx 0.63866$ which is essentially $\bar{\epsilon}^{\mathrm{MAP}}(3,6)$ while the rate loss gradually becomes insignificant. In [11] , Kudekar and Kasai provided a similar plot but here we include the MAP threshold estimate $\bar{\epsilon}^{\mathrm{MAP}}$ and use the EXIT function h^{EBP} instead of the EXIT-like $L(y)$ in [11]. Similarly, one can also verify the threshold

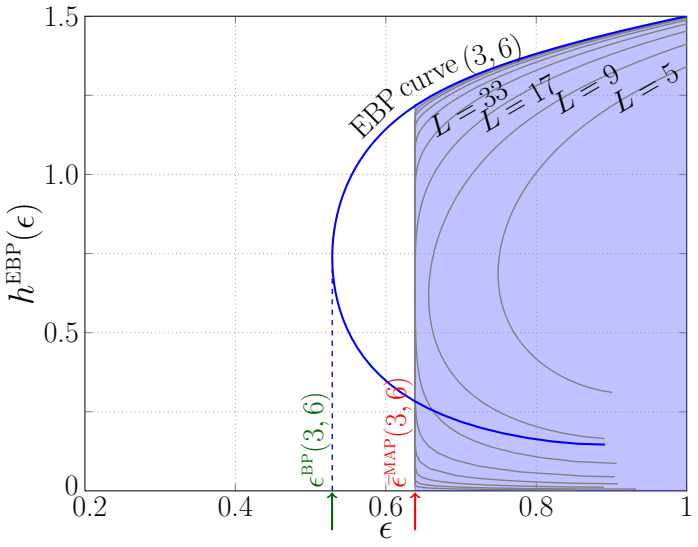

Figure 7. EBP EXIT curves for $(3,6,L,5)$ over the pDEC with $L = 2\hat{L}+1$ where $\hat{L} = 2,4,8,16,32,64,128,246$. Threshold saturation can also be observed for this case.

saturation over the pDEC channel as seen in Fig. 7. For the pDEC, the BP threshold for $(3,6)$-regular ensemble is $\epsilon^{\mathrm{BP}}(3,6) \approx 0.52877$ and by using spatial coupling, the BP threshold can be boosted to $\epsilon^{\mathrm{BP}}(3,6,L,5) \approx \bar{\epsilon}^{\mathrm{MAP}}(3,6) \approx 0.63877$ with negligible rate loss for L large.

Even though the threshold saturation effect has been only shown numerically for the DEC and pDEC, the method is readily applicable to the whole class of GECs. Still, the analytic proof for threshold saturation remains open for the GEC. Such a proof combining with Theorem 2 would essentially demonstrate the SIR-achieving capability of spatially-coupled ensembles.

IV. General ISI Channels

In this section, we shift our focus to ISI channels with more general noise models. The MAP upper bound for general BMS channels was presented by Méasson *et al.* and conjectured to be tight [37]. For general ISI channels, we apply a similar technique to give an estimate of the MAP threshold of the underlying uncoupled ensemble by first constructing the BP-GEXIT curve that follows an area theorem. While our method can be used for a wide range of noise models, we particularly focus on the case of AWGN. The BP thresholds of the corresponding coupled ensembles are then computed via DE and the threshold saturation effect is also observed. In addition, simulations on the performance of the joint BP decoder for coupled codes of finite length are conducted to validate these thresholds.

A. GEXIT Curves for the ISI channels

Consider an ISI channel of memory ν. When the channel input X_1^n is chosen uniformly at random from a suitable binary linear code[7], the ISI output without noise Z_i at some index i is a discrete random variable characterized by its probability mass function $p_{Z_i}(z)$ for all values z in the alphabet $\mathcal{Z}$. For example, in the case of a dicode channel, $\mathcal{Z} = \{0, +2, -2\}$ and $p_{Z_i}(0) = \frac{1}{2}, p_{Z_i}(+2) = p_{Z_i}(-2) = \frac{1}{4}$. The channel from Z_i to Y_i is a $|\mathcal{Z}|$-ary input memoryless channel characterized by its transition probability density $p_{Y_i|Z_i}(y|z)$. Without specifying the index, we denote $\mathtt{h} \triangleq H(Z|Y)$ and get

$$\begin{aligned}\mathtt{h} &= H(Z) - I(Z;Y)\\ &= H(Z) - \int_{-\infty}^{\infty} \sum_z p(z)p(y|z) \log_2 \left\{ \frac{p(y|z)}{\sum_{z'} p(z')p(y|z')} \right\} \mathrm{d}y.\end{aligned}$$

Instead of looking at a particular channel, we assume that the channel from Z_i to Y_i is from a smooth family $\{M(\mathtt{h}_i)\}_{\mathtt{h}_i}$ of $|\mathcal{Z}|$-ary input memoryless channels characterized by conditional entropy $\mathtt{h}_i$. A further assumption is made that all individual channel families are parameterized in a smooth way by a common parameter[8] ϵ, i.e., $\mathtt{h}_i = H(Z_i|Y_i)(\epsilon)$.

With the convention that $y_{\sim i} \triangleq y_1^n \setminus y_i$, define $\phi_i(y_{\sim i}) \triangleq \left\{ P_{Z_i|Y_{\sim i}}(z|y_{\sim i}) : z \in \mathcal{Z} \right\}$ and the random vector $\Phi_i \triangleq \phi_i(Y_{\sim i})$. Each value of ϕ_i is a vector of length $|\mathcal{Z}|$ in the $(|\mathcal{Z}|-1)$-dimensional probability simplex. The index of the vector associated with $z \in \mathcal{Z}$ is denoted by $[z]$. One can see that Φ_i is a sufficient statistic for estimating Z_i, i.e., $Z_i \to \Phi_i(Y_{\sim i}) \to Y_{\sim i}$ forms a Markov chain[9].

Definition 4: Suppose the initial state in the trellis is S_0. Let X_1^n chosen according to $p_{X_1^n}(x_1^n)$ be the input sequence, Z_1^n be the ISI output sequence without noise and Y_1^n be the final channel output sequence, i.e., Y_i is the result of transmitting Z_i over the smooth family $\{M(\mathtt{h}_i)\}_{\mathtt{h}_i}$ of memoryless channels. Then the ith GEXIT function is

$$\mathsf{G}_i(\mathtt{h}_1, \ldots, \mathtt{h}_n) = \frac{\partial H(X_1^n | Y_1^n(\mathtt{h}_1, \ldots, \mathtt{h}_n), S_0)}{\partial \mathtt{h}_i} \tag{26}$$

and the average GEXIT function is defined by

$$\mathsf{G}(\mathtt{h}_1, \ldots, \mathtt{h}_n) = \frac{1}{n} \sum_{i=1}^{n} \mathsf{G}_i(\mathtt{h}_1, \ldots, \mathtt{h}_n).$$

[7]The code is proper [35, p. 14] and its dual code contains no codewords involving only 0's and a run of $(\nu + 1)$ 1's.

[8]For AWGN case, a convenient choice for ϵ is $\epsilon = -\frac{1}{2\sigma^2}$.

[9]One way to see this is to write

$$P_{Y_{\sim i}|Z_i}(y_{\sim i}|z_i) = \frac{P_{Z_i|Y_{\sim i}}(z_i|y_{\sim i})}{P_{Z_i}(z_i)} P_{Y_{\sim i}}(y_{\sim i}) = \frac{\Phi_i \cdot e_{[z_i]}^T}{P_{Z_i}(z_i)} P_{Y_{\sim i}}(y_{\sim i}),$$

where $e_{[z]}^T$ is the standard basis column vector with a 1 in the index $[z]$, and apply the result from [35, p. 29].

For the case where all channel families are the same, i.e., $\mathtt{h}_i = \mathtt{h}$, we have

$$\mathsf{G}(\mathtt{h}) = \frac{1}{n} \cdot \frac{\mathrm{d}H(X_1^n|Y_1^n(\mathtt{h}), S_0)}{\mathrm{d}\mathtt{h}}.$$

Remark 2: The above form of the GEXIT function naturally conforms with the generalized area theorem. Thus, we are able to write the GEXIT curve and use the MAP bounding technique.

Lemma 7: Assume that all the channel families are the same[10], i.e., $\mathtt{h}_i = \mathtt{h}$. The ith GEXIT function is given by

$$\mathsf{G}_i(\mathtt{h}) = \sum_z p(z) \int_{\underline{v}} \mathtt{a}_{i,z}(\underline{v}) \kappa_{i,z}(\underline{v}) \mathrm{d}\underline{v}$$

where $\mathtt{a}_{i,z}$ is the distribution of the vector Φ_i given $Z_i = z$, $\underline{v}$ is a vector of length $|\mathcal{Z}|$ in the $(|\mathcal{Z}| - 1)$-dimensional probability simplex and the GEXIT kernel (for i and z) is[11]

$$\kappa_{i,z}(\underline{v}) = \frac{\int_{-\infty}^{\infty} \frac{\partial}{\partial \epsilon} p(y_i|z) \log_2 \left\{ \frac{\sum_{z'} v_{[z']} p(y_i|z')}{v_{[z]} p(y_i|z)} \right\} \mathrm{d}y_i}{\int_{-\infty}^{\infty} \sum_z p(z) \frac{\partial}{\partial \epsilon} p(y_i|z) \log_2 \left\{ \frac{\sum_{z'} p(z') p(y_i|z')}{p(z) p(y_i|z)} \right\} \mathrm{d}y_i}.$$

Proof: Suppose the initial state is S_0, we start by writing

$$\begin{aligned} H(X_1^n|Y_1^n, S_0) &= H(Z_1^n|Y_1^n, S_0) \\ &= H(Z_i|Y_1^n, S_0) + H(Z_{\sim i}|Y_1^n, Z_i, S_0). \end{aligned} \tag{27}$$

For simplicity of notation, we drop S_0 in all the expressions although the dependency on S_0 is always implied. From (26) and (27), it is clear that

$$\mathsf{G}_i(\mathtt{h}) = \frac{\partial}{\partial \mathtt{h}_i} H(Z_i|Y_1^n). \tag{28}$$

We also have

$$\begin{aligned} H(Z_i|Y_1^n) &= H(Z_i|Y_i, \Phi_i(Y_{\sim i})) \\ &= -\int_{\phi_i} \int_{y_i} \sum_{z_i} p(z_i) p(\phi_i|z_i) p(y_i|z_i) \log_2 \left\{ \frac{p(z_i|\phi_i) p(y_i|z_i)}{\sum_{z_i'} p(z_i'|\phi_i) p(y_i|z_i')} \right\} \mathrm{d}y_i \mathrm{d}\phi_i \end{aligned} \tag{29}$$

where (29) follows from the Bayes' theorem and the fact that

$$p(z_i, \phi_i, y_i) = p(z_i, \phi_i) p(y_i|\phi_i, z_i) = p(z_i) p(\phi|z_i) p(y_i|z_i). \tag{30}$$

[10]Note that for the case of different channel families, one can still compute the ith GEXIT function as a function of the common parameter ϵ.

[11]$p(y_i|z)$ is dependent on $\mathtt{h}_i$ and hence is dependent on ϵ.

Note that (30) is true since Y_i and $\Phi_i(Y_{\sim i})$ are independent given Z_i, i.e., $Y_i \to Z_i \to \Phi_i(Y_{\sim i})$.

Taking derivative and using $p(z_i|\phi_i) = p(z_i|y_{\sim i})$, we get[12]

$$\begin{aligned}\mathsf{G}_i(\mathtt{h}) &= \sum_{z_i} p(z_i) \int_{\phi_i} p(\phi_i|z_i) \int_{y_i} \frac{\mathrm{d}}{\mathrm{d}\mathtt{h}_i} p(y_i|z_i) \log_2 \left\{ \sum_{z_i'} \frac{p(z_i'|y_{\sim i}) p(y_i|z_i')}{p(z_i|y_{\sim i}) p(y_i|z_i)} \right\} \mathrm{d}y_i \mathrm{d}\phi_i \\ &= \sum_{z} p(z) \int_{\underline{v}} \mathsf{a}_{i,z}(\underline{v}) \kappa_{i,z}(\underline{v}) \mathrm{d}\underline{v}.\end{aligned}$$

where

$$\begin{aligned}\kappa_{i,z}(\underline{v}) &= \int_{y_i} \frac{\mathrm{d}}{\mathrm{d}\mathtt{h}_i} p(y_i|z) \log_2 \left\{ \frac{\sum_{z'} v_{[z']} p(y_i|z')}{v_{[z]} p(y_i|z)} \right\} \mathrm{d}y_i \\ &= \int_{y_i} \frac{\partial}{\partial \epsilon} p(y_i|z) \log_2 \left\{ \frac{\sum_{z'} v_{[z']} p(y_i|z')}{v_{[z]} p(y_i|z)} \right\} \mathrm{d}y_i \Big/ \frac{\partial \mathtt{h}_i}{\partial \epsilon}.\end{aligned}$$

Finally, by seeing that

$$\begin{aligned}\frac{\partial \mathtt{h}_i}{\partial \epsilon} &= \frac{\partial H(Z_i|Y_i(\epsilon))}{\partial \epsilon} \\ &= \sum_{z} \int_{y_i} p(z) \frac{\partial}{\partial \epsilon} p(y_i|z) \log_2 \left\{ \frac{\sum_{z'} p(z') p(y_i|z')}{p(z) p(y_i|z)} \right\} \mathrm{d}y_i.\end{aligned}$$

we obtain the result. ∎

Remark 3: For erasure noise and the GEC in particular, $\mathtt{h} = H(Z|Y) = \epsilon H(Z)$ (scaling ϵ by $H(Z)$) and since in this case

$$\kappa_{i,z}(\underline{v}) = \frac{1}{H(Z)} \log_2 \left\{ 1 + \frac{\sum_{z' \neq z} v_{[z']}}{v_{[z]}} \right\},$$

$\mathsf{G}(\mathtt{h}) = \frac{h(\epsilon)}{H(Z)}$ (scaling $h(\epsilon)$ by $\frac{1}{H(Z)}$) where $h(\epsilon)$ is the EXIT function for the GEC.

Remark 4: At $\sigma = 0$ for AWGN case (or at $\epsilon = 0$ for erasure noise), $\mathtt{h} = 0$ and $\mathsf{a}_{i,z}$ is "delta at $\underline{v} = e_{[z]}$" where $e_{[z]}$ is the standard basis vector. At this extreme, $\mathsf{G}(0) = 0$ since $\kappa_{i,z}(\underline{v}) = 0$. At the other extreme $\sigma \to \infty$ (or at $\epsilon = 1$ for erasure noise), $\mathtt{h} = H(Z)$ (e.g., 1.5 for the dicode channel) and $\mathsf{G}(\mathtt{h}) = 1$ since in this case $\mathsf{a}_{i,z}$ is "delta at $v_{[z']} = p(z')\ \forall z'$".

1) BP-GEXIT curve (with AWGN): In this section, we are particularly interested in computing the BP-GEXIT function for ISI channels with AWGN. In this case, let $\Phi_i^{\mathrm{BP},\ell}$ denote the extrinsic estimate of Z_i at the ℓth round of joint BP decoding. If $\Phi_i^{\mathrm{BP},\ell}$ is used instead of Φ_i in the above formulas then one has the BP-GEXIT (at the ℓth round) $\mathsf{G}^{\mathrm{BP},\ell}$ in a similar manner to [37] and the overall BP-GEXIT $\mathsf{G}^{\mathrm{BP}}(\mathtt{h}) = \lim_{\ell \to \infty} \mathsf{G}^{\mathrm{BP},\ell}(\mathtt{h})$. Also, notice that the two extremes in Remark 4 still apply when the BP decoder is used instead of the MAP decoder.

[12]One can verify that the terms obtained by taking derivative with respect to the channel inside the $\log_2$ vanish.

Next, AWGN implies that $p(y_i|z) = \frac{1}{\sqrt{2\pi\sigma^2}} e^{-\frac{(y_i-z)^2}{2\sigma^2}}$ and then $\frac{\partial}{\partial \epsilon} p(y_i|z) = ((y_i - z)^2 - \sigma^2) p(y_i|z)$. Therefore, the corresponding ith BP-GEXIT is $\mathsf{G}_i^{\mathrm{BP},\ell}(\mathsf{h}) = \frac{A}{B}$ where

$$A = \sum_z p(z) \int_{\underline{v}} \mathsf{a}_{i,z}^{\mathrm{BP},\ell}(\underline{v}) \int_{-\infty}^{\infty} p(y_i|z) \left\{ \frac{(y_i - z)^2}{\sigma^2} - 1 \right\} \log_2 \left\{ \sum_{z'} \frac{v_{[z']}}{v_{[z]}} e^{\frac{(z'-z)(2y_i - z - z')}{2\sigma^2}} \right\} \mathrm{d}y_i \mathrm{d}\underline{v}$$

and

$$B = \sum_z p(z) \int_{-\infty}^{\infty} p(y_i|z) \left\{ \frac{(y_i - z)^2}{\sigma^2} - 1 \right\} \log_2 \left\{ \sum_{z'} \frac{p(z')}{p(z)} e^{\frac{(z'-z)(2y_i - z - z')}{2\sigma^2}} \right\} \mathrm{d}y_i.$$

In the limit of $\ell \to \infty$, one can run the DE for ISI channels [15] to obtain the DE-FP and compute the quantities A and B at this FP. With some abuse of notation, let $\mathsf{a}^{(\ell)}, \mathsf{b}^{(\ell)}, \mathsf{c}^{(\ell)}$ and $\mathsf{d}^{(\ell)}$ denote the average density of the bit-to-check, check-to-bit, bit-to-trellis and trellis-to-bit messages, respectively (see Fig. 1), at iteration ℓ with initial values (at $\ell = 0$) being Δ_0, the delta function at 0. Also, let n denote the density of channel noise. The DE update equation for joint BP decoding of a general binary-input ISI channels is

$$\begin{aligned}
\mathsf{a}^{(\ell)} &= \mathsf{d}^{(\ell-1)} \circledast \lambda(\mathsf{b}^{(\ell-1)}), \\
\mathsf{b}^{(\ell)} &= \rho(\mathsf{a}^{(\ell)}), \\
\mathsf{c}^{(\ell)} &= L(\mathsf{b}^{(\ell)}), \\
\mathsf{d}^{(\ell)} &= \Gamma(\mathsf{c}^{(\ell)}, \mathsf{n})
\end{aligned}$$

where for a density x, $\lambda(\mathsf{x}) = \sum_i \lambda_i \mathsf{x}^{\circledast(i-1)}$, $\rho(\mathsf{x}) = \sum_i \rho_i \mathsf{x}^{\boxtimes(i-1)}$ and $L(\mathsf{x}) = \sum_i L_i \mathsf{x}^{\circledast i}$. The operators $\circledast$ and $\boxtimes$ are the standard density transformations used in [35, p. 181]. The map $\Gamma(\cdot,\cdot)$ is not easy to compute in closed form for general trellises and often one needs to resort to the Monte Carlo methods (i.e., running the windowed BCJR algorithm with window parameter W on a long enough trellis - see details in [15]) to give the estimates. A similar method was used to upper bound the MAP threshold for turbo codes over BMS channels [38].

The denominator B can be computed either by numerical integration or by Monte Carlo methods. Meanwhile, the numerator A involves in the quantity $v_{[z]} = p\left(Z_i = z | \mathtt{T}_i^\ell\right)$ where $\mathtt{T}_i^\ell$ denotes the computation tree of depth ℓ, rooted at index i, which includes all channel and code constraints associated with ℓ iterations of decoding. This computation tree $\mathtt{T}_i^\ell$ excludes the tree root y_i and is implied by the decoding schedule in the DE equation. The quantity $v_{[z]}$, due to complications from the trellis, is not easy to obtain in closed form. However, one can readily compute $v_{[z]}$ as an extra output of the BCJR algorithm (already used in DE) as

$$v_{[z]} \propto \sum_{s_i, s_{i-1}: Z_i = z} \alpha_{i-1}(s_{i-1}) \cdot \gamma_i(s_{i-1}, s_i) \cdot \beta_i(s_i).$$

where $\gamma_i(s_{i-1}, s_i)$ is probability of the input x_i that corresponds to the transition from state s_{i-1} (at time index $i-1$) to state s_i at (time index i) given the computation tree $\mathtt{T}_i^\ell$. Here, $\alpha_i(\cdot)$ and $\beta_i(\cdot)$ are the standard forward and backward state probabilities in the BCJR algorithm. Note that the scaling constant can be chosen so that $\sum_z v_{[z]} = 1$.

B. Upper Bound for the MAP Threshold

As briefly discussed before, the above-mentioned GEXIT curve naturally follows the area theorem

$$\int_{\mathtt{h}^{\mathrm{MAP}}}^{H(Z)} \mathsf{G}(\mathtt{h})\mathrm{d}\mathtt{h} = \int_{0}^{H(Z)} \mathsf{G}(\mathtt{h})\mathrm{d}\mathtt{h} = \mathtt{r}.$$

One can also apply [37, Lm. 4] to the BMS channel from Z_1^n to Y_1^n and obtains

$$\frac{\partial H(Z_i|Y_1^n)}{\partial \mathtt{h}_i} \leq \frac{\partial H(Z_i|Y_i, \Phi_i^{\mathrm{BP},\ell})}{\partial \mathtt{h}_i}.$$

Consequently, by invoking (28), one has the optimality of the MAP decoder in the sense that $\mathsf{G}(\mathtt{h}) \leq \mathsf{G}^{\mathrm{BP}}(\mathtt{h})$. Therefore, one can use the discussed bounding technique, i.e., by finding the largest value $\bar{\mathtt{h}}^{\mathrm{MAP}}$ such that the area under the BP-GEXIT curve equals the code rate,

$$\int_{\bar{\mathtt{h}}^{\mathrm{MAP}}}^{H(Z)} \mathsf{G}^{\mathrm{BP}}(\mathtt{h})\mathrm{d}\mathtt{h} = \mathtt{r},$$

to obtain the MAP upper bound $\bar{\mathtt{h}}^{\mathrm{MAP}} \geq \mathtt{h}^{\mathrm{MAP}}$ (as $\int_{\bar{\mathtt{h}}^{\mathrm{MAP}}}^{H(Z)} \mathsf{G}^{\mathrm{BP}}(\mathtt{h})\mathrm{d}\mathtt{h} = \int_{\mathtt{h}^{\mathrm{MAP}}}^{H(Z)} \mathsf{G}(\mathtt{h})\mathrm{d}\mathtt{h} \leq \int_{\mathtt{h}^{\mathrm{MAP}}}^{H(Z)} \mathsf{G}^{\mathrm{BP}}(\mathtt{h})\mathrm{d}\mathtt{h}$).

For example, the BP-GEXIT curve for the $(3,6)$-regular LDPC code over an AWGN dicode channel with $a(D) = (1-D)/\sqrt{2}$ following the analysis in Section IV-A is shown in Fig. 8. In this case, $\mathtt{h}^{\mathrm{BP}}(3,6) \approx 0.851 \pm 0.001$ (the corresponding[13] $\sigma^{\mathrm{BP}}(3,6) \approx 1.703 \pm 0.001$ dB) while $\bar{\mathtt{h}}^{\mathrm{MAP}}(3,6) \approx 0.920 \pm 0.001$ (or $\bar{\sigma}^{\mathrm{MAP}}(3,6) \approx 0.959 \pm 0.001$ dB). Similarly, for the $(5,10)$-regular LDPC code, one has $\mathtt{h}^{\mathrm{BP}}(5,10) \approx 0.716 \pm 0.001$ and $\bar{\mathtt{h}}^{\mathrm{MAP}}(5,10) \approx 0.931 \pm 0.001$. The corresponding thresholds measured in dB can be found in Table. I.

C. Spatially-Coupled Codes on the ISI Channels

Consider the (l, r, L) spatially-coupled ensemble. For the ISI channels, the DE equation for this ensemble can be obtained from the protograph chain in a similar manner to the case of memoryless channels discussed in [39]. For each $i, j \in [1-\hat{l}, L+\hat{l}]$, let $\mathtt{a}_{i\to j}^{(\ell)}$ (and $\mathtt{b}_{i\leftarrow j}^{(\ell)}$) denote the average density

[13]We adopt the convention that σ is the SNR threshold measured in dB.

(l,r)-regular	DEC			Dicode AWGN		
	ϵ^{BP}	$\bar{\epsilon}^{\text{MAP}}$	ϵ^{SIR}	σ^{BP}	$\bar{\sigma}^{\text{MAP}}$	σ^{SIR}
$(3,6)$	0.5689	0.6387	0.6404	1.073	0.959	0.823
$(5,10)$	0.4647	0.6404	0.6404	3.032	0.834	0.823

Table I

THRESHOLD ESTIMATES OF (l,r)-REGULAR ENSEMBLES OVER THE DEC AND DICODE AWGN CHANNEL. FOR AWGN NOISE, THE THRESHOLDS ARE MEASURED IN DB.

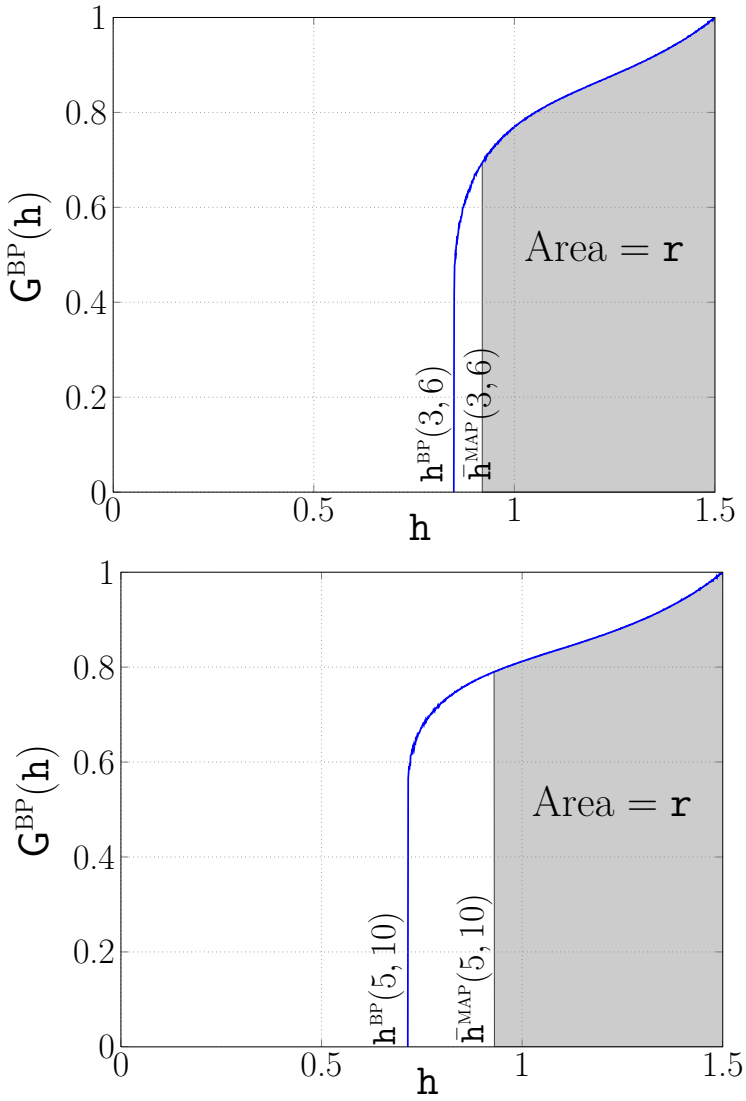

Figure 8. The BP-GEXIT curve for $(3,6)$-regular and $(5,10)$-regular LDPC codes over an AWGN dicode channel with $a(D) = (1-D)/\sqrt{2}$. The upper bound $\bar{\mathtt{h}}^{\text{MAP}}$ is obtained by setting the area under the BP-GEXIT curve (the shaded region) equal to the code rate.

of the messages from bit nodes at position i to check nodes at position j (and the other way around)[14]. With all the initial message densities (at $\ell = 0$) being Δ_0, the DE update equation (for all $i \in [1, L]$) is

$$\begin{aligned}
\mathsf{a}_{i\to j}^{(\ell)} &= \mathsf{d}_i^{(\ell-1)} \circledast \left\{ \underset{j'\in[i-\hat{l},i+\hat{l}]\setminus j}{\circledast} \mathsf{b}_{i\leftarrow j'}^{(\ell-1)} \right\}, \forall j \in [i-\hat{l}, i+\hat{l}], \\
\mathsf{b}_{i\leftarrow j}^{(\ell)} &= \underset{i'\in[j-\hat{l},j+\hat{l}]\setminus i}{\circledast} \mathsf{a}_{i'\to j}^{(\ell)}, \forall j \in [i-\hat{l}, i+\hat{l}], \\
\mathsf{c}_i^{(\ell)} &= \underset{j'\in[i-\hat{l},i+\hat{l}]}{\circledast} \mathsf{b}_{i\leftarrow j'}^{(\ell)}, \\
\mathsf{d}_i^{(\ell)} &= \Gamma(\mathsf{c}_i^{(\ell)}, \mathsf{n})
\end{aligned}$$

where $\circledast_{j\in\{j_1,\ldots,j_t\}} \mathsf{x}_j$ and $\circledcirc_{i\in\{i_1,\ldots,i_t\}} \mathsf{x}_i$ denote the operations $\mathsf{x}_{j_1} \circledast \mathsf{x}_{j_2} \circledast \ldots \circledast \mathsf{x}_{j_t}$ and $\mathsf{x}_{i_1} \circledcirc \mathsf{x}_{i_2} \circledcirc \ldots \circledcirc \mathsf{x}_{i_t}$, respectively.

D. Simulation Results

In this section, we start with the (l, r, L) circular ensemble obtained by considering all the positions $i > L$ of the protograph chain to be the same as position $i-L$ (similar to [8]). The order of bit transmissions is "left to right" in each length-L row and then start with the next row (in a total of M rows, see Fig. 2). The $I \triangleq \max(\nu, l-1)$ first bits in each row are known. This known bits will "break" the circular ensemble into the $(l, r, L-I)$ ensemble and also serve as the pilot bits to fix the trellis state. As a consequence of this fixing, one only needs to run the BCJR independently in each row and this can be done in a parallel manner [22], [23].

In our experiments, we conduct simulations over the AWGN dicode channel with $a(D) = (1-D)/\sqrt{2}$ and memory $\nu = 1$. First, we use the DE in Sec. IV-C to compute the BP thresholds of the spatially-coupled coding scheme. The results in Fig. 9 reveals that $\sigma^{\mathrm{BP}}(3, 6, 22)$ is roughly 0.959 ± 0.001 dB and approximately the same as $\sigma^{\mathrm{BP}}(3, 6, 44)$ whose rate loss is smaller. Notice that this is also roughly $\bar{\sigma}^{\mathrm{MAP}}(3, 6)$ - the MAP threshold estimate of the underlying $(3, 6)$-regular ensemble, obtained by the bounding technique, and is a significant improvement over $\sigma^{\mathrm{BP}}(3, 6) \approx 1.703 \pm 0.001$ dB. This suggests that threshold saturation occurs for regular ensembles. Since MAP decoding of regular ensembles can achieve the SIR [27], it also implies that one can universally approach the SIR of general ISI channels using coupled codes with joint iterative decoding. To support this, one can also see that for the $(5, 10, 44)$

[14]For $i \notin [1, L]$, set $\mathsf{a}_{i\to j}^{(\ell)} = \Delta_{+\infty}$, the delta function at $+\infty$.

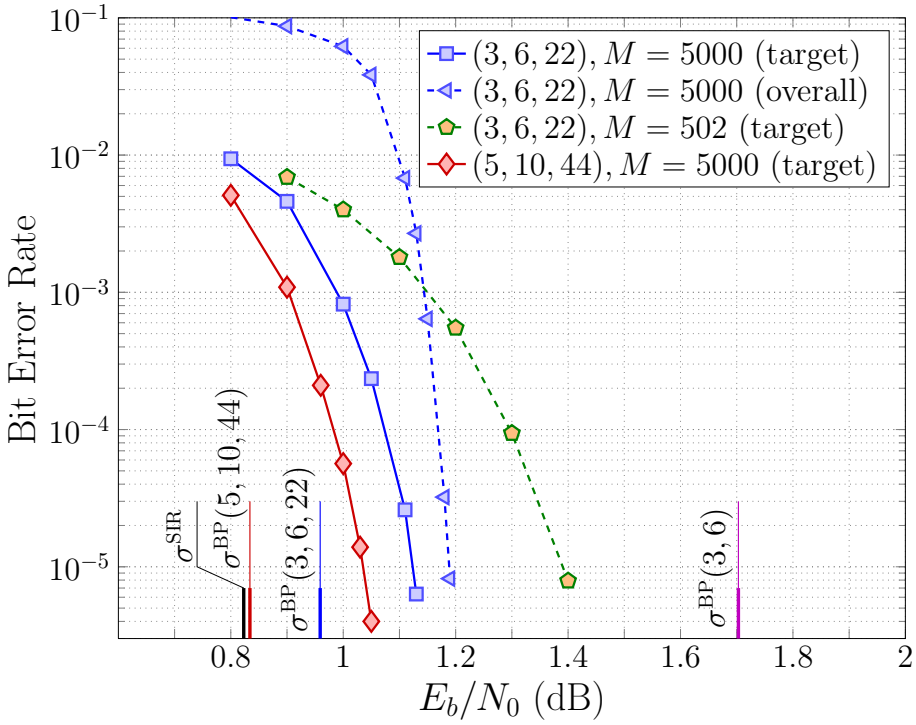

Figure 9. BER and BP thresholds for the $(3,6)$-regular LDPC code, $(3,6,22)$ and $(5,10,44)$ spatially-coupled codes over the AWGN dicode channel.

ensemble of the same rate as the $(3,6,22)$ one, the threshold $\sigma^{\mathrm{BP}}(5,10,44) \approx 0.834 \pm 0.001$ dB (which is also roughly $\bar{\sigma}^{\mathrm{MAP}}(5,10)$) gets very close to the signal-to-noise ratio (SNR) corresponding to the SIR ($\sigma^{\mathrm{SIR}} \approx 0.823 \pm 0.001$ dB using the numerical method in [16], [17]).

Also shown in Fig. 9 is the bit error rate (BER) versus SNR plot for the ensembles derived from the (l,r,L) circular ensembles of finite M = 502 and M = 5000. For each simulation, we use $\mathtt{l}_{\mathrm{outer}}$ = 20 channel updates and between two such channel updates, we run $\mathtt{l}_{\mathrm{inner}}$ = 5 BP iterations on the code part alone. The curves labeled "target" is the BER for the bits at position $I+1$ (right after the known bits) in the coupled chain while the curve labeled "overall" is the overall BER for all the positions $[I+1, L]$ together. One might expect that the "overall" BER will get closer to the "target" BER for large enough M and large enough number of iterations. From Fig. 9, one can also observe that the "overall" BER for $(3,6,22)$ and M = 5000 keeps getting "closer" to the "target" BER as SNR slightly increases. Those BER curves are way to the left of $\epsilon^{\mathrm{BP}}(3,6)$ - the BP threshold for the underlying $(3,6)$-regular ensemble.

V. Concluding Remarks

In this paper, we consider binary communication over the ISI channels and numerically show that the threshold saturation effect occurs on both the DEC and dicode channel with AWGN. To do this, we construct the EXIT and GEXIT curves that satisfy the area theorem and obtain an upper bound on the threshold of the MAP decoder. This upper bound is conjectured to be tight and, for the DEC, we show a numerical evidence which strongly supports this conjecture. The observed threshold saturation effect is valuable because by changing the underlying regular LDPC ensemble, i.e., increasing the degrees according to a fixed code rate, combined with the results of [27], it is shown that the joint BP decoding of spatially-coupled codes can universally approach the SIR of the ISI channels.

Also, it has been known that the spatially-coupled codes (or LDPC convolutional codes) inherit some other advantages such as the typical minimum distance and the size of the smallest non-empty trapping sets both growing linearly with the protograph expansion M [40]. In addition, the convolutional structure of the codes allows one to consider a windowed decoder like the one discussed in [41], [42]. All of these properties suggest that spatially-coupled codes may be competitive in practice for systems with ISI.

References

[1] M. G. Luby, M. Mitzenmacher, M. A. Shokrollahi, and D. A. Spielman, "Efficient erasure correcting codes," *IEEE Trans. Inform. Theory*, vol. 47, no. 2, pp. 569–584, Feb. 2001.

[2] S. Chung, G. D. Forney, Jr., T. J. Richardson, and R. L. Urbanke, "On the design of low-density parity-check codes within 0.0045 dB of the Shannon limit," *IEEE Commun. Letters*, vol. 5, no. 2, pp. 58–60, Feb. 2001.

[3] J. Felstrom and K. S. Zigangirov, "Time-varying periodic convolutional codes with low-density parity-check matrix," *IEEE Trans. Inform. Theory*, vol. 45, no. 6, pp. 2181–2191, 1999.

[4] A. Sridharan, M. Lentmaier, D. J. Costello, and K. S. Zigangirov, "Convergence analysis of a class of LDPC convolutional codes for the erasure channel," in *Proc. Annual Allerton Conf. on Commun., Control, and Comp.*, Monticello, IL, 2004, pp. 953–962.

[5] M. Lentmaier, A. Sridharan, K. Zigangirov, and D. J. Costello, "Terminated LDPC convolutional codes with thresholds close to capacity," in *Proc. IEEE Int. Symp. Inform. Theory*, Adelaide, Australia, 2005, pp. 1372–1376.

[6] S. Kudekar, T. Richardson, and R. Urbanke, "Threshold saturation via spatial coupling: Why convolutional LDPC ensembles perform so well over the BEC," *IEEE Trans. Inform. Theory*, vol. 57, no. 2, pp. 803–834, 2011.

[7] M. Lentmaier and G. Fettweis, "On the thresholds of generalized LDPC convolutional codes based on protographs," in *Proc. IEEE Int. Symp. Inform. Theory*, Austin, TX, 2010, pp. 709–713.

[8] S. Kudekar, C. Méasson, T. Richardson, and R. Urbanke, "Threshold saturation on BMS channels via spatial coupling," in *Proc. Int. Symp. on Turbo Codes & Iterative Inform. Proc.*, Sept. 2010, pp. 309–313.

[9] S. Kudekar and H. Pfister, "The effect of spatial coupling on compressive sensing," in *Proc. Annual Allerton Conf. on Commun., Control, and Comp.*, Monticello, IL, Oct. 2010, pp. 347–353.

[10] S. Hassani, N. Macris, and R. Urbanke, "Coupled graphical models and their thresholds," in *Proc. IEEE Inform. Theory Workshop*, Dublin, Ireland, 2010, pp. 1–5.

[11] S. Kudekar and K. Kasai, "Threshold saturation on channels with memory via spatial coupling," in *Proc. IEEE Int. Symp. Inform. Theory*, St. Petersburg, Russia, July 2011, pp. 2562–2566.

[12] ——, "Spatially coupled codes over the multiple access channel," in *Proc. IEEE Int. Symp. Inform. Theory*, St. Petersburg, Russia, July 2011, pp. 2816–2820.

[13] A. Yedla, H. Pfister, and K. Narayanan, "Universality for the noisy Slepian-Wolf problem via spatial coupling," in *Proc. IEEE Int. Symp. Inform. Theory*, St. Petersburg, Russia, July 2011, pp. 2567–2571.

[14] A. Yedla, P. S. Nguyen, H. D. Pfister, and K. R. Narayanan, "Universal codes for the Gaussian MAC via spatial coupling," in *Proc. Annual Allerton Conf. on Commun., Control, and Comp.*, Monticello, IL, Sept. 2011.

[15] A. Kavčić, X. Ma, and M. Mitzenmacher, "Binary intersymbol interference channels: Gallager codes, density evolution and code performance bounds," *IEEE Trans. Inform. Theory*, vol. 49, no. 7, pp. 1636–1652, July 2003.

[16] D. Arnold and H. Loeliger, "On the information rate of binary-input channels with memory," in *Proc. IEEE Int. Conf. Commun.*, Helsinki, Finland, June 2001, pp. 2692–2695.

[17] H. D. Pfister, J. B. Soriaga, and P. H. Siegel, "On the achievable information rates of finite state ISI channels," in *Proc. IEEE Global Telecom. Conf.*, San Antonio, Texas, USA, Nov. 2001, pp. 2992–2996.

[18] B. M. Kurkoski, P. H. Siegel, and J. K. Wolf, "Joint message-passing decoding of LDPC codes and partial-response channels," *IEEE Trans. Inform. Theory*, vol. 48, no. 6, pp. 1410–1422, June 2002.

[19] H. D. Pfister and P. H. Siegel, "Joint iterative decoding of LDPC codes and channels with memory," in *Proc. 3rd Int. Symp. on Turbo Codes & Related Topics*, Brest, France, Sept. 2003, pp. 15–18.

[20] ——, "Joint iterative decoding of LDPC codes for channels with memory and erasure noise," *IEEE J. Select. Areas Commun.*, vol. 26, no. 2, pp. 320–337, Feb. 2008.

[21] N. Varnica and A. Kavčić, "Optimized low-density parity-check codes for partial response channels," *IEEE Commun. Letters*, vol. 7, no. 4, pp. 168–170, 2003.

[22] K. R. Narayanan and N. Nangare, "A BCJR-DFE based receiver for achieving near capacity performance on inter symbol interference channels," in *Proc. 43rd Annual Allerton Conf. on Commun., Control, and Comp.*, Monticello, IL, Oct. 2004, pp. 763–772.

[23] J. B. Soriaga, H. D. Pfister, and P. H. Siegel, "Determining and approaching achievable rates of binary intersymbol interference channels using multistage decoding," *IEEE Trans. Inform. Theory*, vol. 53, no. 4, pp. 1416–1429, April 2007.

[24] H. D. Pfister, "On the capacity of finite state channels and the analysis of convolutional accumulate-m codes," Ph.D. dissertation, University of California, San Diego, La Jolla, CA, USA, March 2003.

[25] C. Méasson, A. Montanari, and R. L. Urbanke, "Maxwell construction: The hidden bridge between iterative and maximum a posteriori decoding," *IEEE Trans. Inform. Theory*, vol. 54, no. 12, pp. 5277–5307, Dec. 2008.

[26] C. Wang and H. D. Pfister, "Upper bounds on the MAP threshold of iterative decoding systems with erasure noise," in *Proc. Int. Symp. on Turbo Codes & Related Topics*, Lausanne, Switzerland, Sept. 2008, pp. 7–12.

[27] J. H. Bae and A. Anastasopoulos, "Capacity-achieving codes for finite-state channels with maximum-likelihood decoding," *IEEE J. Select. Areas Commun.*, vol. 27, no. 6, pp. 974–984, Aug. 2009.

[28] L. R. Bahl, J. Cocke, F. Jelinek, and J. Raviv, "Optimal decoding of linear codes for minimizing symbol error rate," *IEEE Trans. Inform. Theory*, vol. 20, no. 2, pp. 284–287, March 1974.

[29] D. Arnold, H. A. Loeliger, P. O. Vontobel, A. Kavčić, and W. Zeng, "Simulation-based computation of information rates for channels with memory," *IEEE Trans. Inform. Theory*, vol. 52, no. 8, pp. 3498–3508, Aug. 2006.

[30] C. Douillard, M. Jézéquel, C. Berrou, A. Picart, P. Didier, and A. Glavieux, "Iterative correction of intersymbol interference: Turbo equalization," *Eur. Trans. Telecom.*, vol. 6, no. 5, pp. 507–511, Sept. – Oct. 1995.

[31] J. Hou, P. H. Siegel, L. B. Milstein, and H. D. Pfister, "Capacity-approaching bandwidth-efficient coded modulation schemes based on low-density parity-check codes," *IEEE Trans. Inform. Theory*, vol. 49, no. 9, pp. 2141–2155, Sept. 2003.

[32] T. M. Cover and J. A. Thomas, *Elements of Information Theory*, ser. Wiley Series in Telecommunications. Wiley, 1991.

[33] A. Ashikhmin, G. Kramer, and S. ten Brink, "Extrinsic information transfer functions: model and erasure channel properties," *IEEE Trans. Inform. Theory*, vol. 50, no. 11, pp. 2657–2674, Nov. 2004.

[34] C. Méasson, A. Montanari, and R. Urbanke, "Asymptotic rate versus design rate," in *Proc. IEEE Int. Symp. Inform. Theory*, Nice, France, June 2007, pp. 1541–1545.

[35] T. J. Richardson and R. L. Urbanke, *Modern Coding Theory*. Cambridge, 2008.

[36] H. D. Pfister and I. Sason, "Accumulate–repeat–accumulate codes: Capacity-achieving ensembles of systematic codes for the erasure channel with bounded complexity," *IEEE Trans. Inform. Theory*, vol. 53, no. 6, pp. 2088–2115, June 2007.

[37] C. Méasson, A. Montanari, T. Richardson, and R. Urbanke, "The generalized area theorem and some of its consequences," *IEEE Trans. Inform. Theory*, vol. 55, no. 11, pp. 4793–4821, Nov. 2009.

[38] ——, "Maximum a posteriori decoding and turbo codes for general memoryless channels," in *Proc. IEEE Int. Symp. Inform. Theory*, Adelaide, Australia, 2005, pp. 1241–1245.

[39] M. Lentmaier, A. Sridharan, D. J. Costello, and K. S. Zigangirov, "Iterative decoding threshold analysis for LDPC convolutional codes," *IEEE Trans. Inform. Theory*, vol. 56, no. 10, pp. 5274–5289, Oct. 2010.

[40] D. G. M. Mitchell, A. E. Pusane, M. Lentmaier, and D. J. Costello, "Exact free distance and trapping set growth rates for LDPC convolutional codes," in *Proc. IEEE Int. Symp. Inform. Theory*, St. Petersburg, Russia, July 2011, pp. 1096–1100.

[41] A. R. Iyengar, M. Papaleo, P. H. Siegel, J. K. Wolf, A. Vanelli-Coralli, and G. E. Corazza, "Windowed decoding of protograph-based LDPC convolutional codes over erasure channels," Oct. 2010, submitted to *IEEE Trans. on Inform. Theory* [Online]. Available: http://arxiv.org/abs/1010.4548.

[42] A. R. Iyengar, P. H. Siegel, R. L. Urbanke, and J. K. Wolf, "Windowed decoding of spatially coupled codes," in *Proc. IEEE Int. Symp. Inform. Theory*, St. Petersburg, Russia, July 2011, pp. 2552–2556.